

## MODULE 2.6.4. PHARMACOKINETICS WRITTEN SUMMARY

This document contains confidential information belonging to BioNTech/Pfizer. Except as may be otherwise agreed to in writing, by accepting or reviewing these materials, you agree to hold such information in confidence and not to disclose it to others (except where required by applicable law), nor to use it for unauthorized purposes. In the event of actual or suspected breach of this obligation, BioNTech/Pfizer should be promptly notified.

## TABLE OF CONTENTS

LIST OF ABBREVIATIONS AND DEFINITION OF TERMS .....	3
2.6.4. PHARMACOKINETICS WRITTEN SUMMARY .....	4
2.6.4.1. Brief Summary .....	4
2.6.4.2. Methods of Analysis.....	5
2.6.4.3. Absorption .....	5
2.6.4.4. Distribution.....	6
2.6.4.5. Metabolism.....	8
2.6.4.6. Excretion .....	10
2.6.4.7. Pharmacokinetic Drug Interactions .....	10
2.6.4.8. Discussion and Conclusions .....	10
2.6.4.9. References .....	11

## LIST OF ABBREVIATIONS AND DEFINITION OF TERMS

ADME	Absorption, distribution, metabolism, excretion
ALC-0159	Proprietary PEG-lipid included as an excipient in the LNP formulation used in BNT162b2
ALC-0315	Proprietary amino-lipid included as an excipient in the LNP formulation used in BNT162b2
BLI	Bioluminescence imaging
[ <sup>3</sup> H]-CHE	Radiolabeled [Cholesteryl-1,2- <sup>3</sup> H(N)]-Cholesteryl Hexadecyl Ether
DSPC	1,2-distearoyl-sn-glycero-3-phosphocholine
GFP	Green fluorescent protein
GLP	Good Laboratory Practice
H	Human (in metabolite scheme)
HPD	Hours post dose
IHC	Immunohistochemistry
IM	Intramuscular(ly)
ISH	In situ hybridization
IV	Intravenous(ly)
LNP	Lipid-nanoparticle
Luc	Luciferase (from firefly <i>Pyroactomena lucifera</i> )
Mk	Monkey (in metabolite scheme)
Mo	Mouse (in metabolite scheme)
modRNA	Nucleoside-modified mRNA
mRNA	Messenger RNA
PEG	Polyethylene glycol
PK	Pharmacokinetics
R	Rat (in metabolite scheme)
RNA	Ribonucleic acid
S9	Supernatant fraction obtained from liver homogenate by centrifuging at 9000 g
WHO	World Health Organization

## 2.6.4. PHARMACOKINETICS WRITTEN SUMMARY

### 2.6.4.1. Brief Summary

The ADME profile of BNT162b2 (BioNTech code number BNT162, Pfizer code number PF-07302048) included evaluation of the PK and metabolism of two novel lipid excipients (ALC-0315 and ALC-0159) in the LNP and potential biodistribution using luciferase or GFP as a surrogate reporter or a radiolabeled lipid marker. Biodistribution of BNT162b2 mRNA and its translation to spike protein were also assessed.

The PK study showed the LNP distributes from the blood to the liver, ~1% of ALC-0315 and ~50% of ALC-0159 were excreted unchanged in feces, and there was no detectable excretion of unchanged ALC-0315 and ALC-0159 in the urine.

In a mouse biodistribution study, protein expression was demonstrated at the site of injection and to a lesser extent in the liver after BALB/c mice received an IM injection of modRNA encoding luciferase in an LNP formulation, with the identical lipid composition as BNT162b2. Luciferase expression was identified at the injection site at 6 HPD and was not detected after 9 days. Liver expression was also present at 6 HPD and was no longer detected by 48 HPD. A quantitative biodistribution study was also carried out in Wistar Han rats using a radiolabeled lipid marker and a luciferase modRNA in the same LNP formulation as BNT162b2. Following IM administration, the greatest mean concentration remained at the injection site, while up to 18% of the administered dose was found in the liver. Another study utilizing the luciferase reporter identified the injection site (muscle) and the closest draining lymph node (popliteal) as the main sites of luciferase expression with additional draining lymph nodes on the injection side of the body, liver, and spleen all showing low expression.

The cellular distribution and protein expression of the modRNA-LNP platform of BNT162b2 were evaluated in CD-1 male mice following IM injection of GFP modRNA-LNP. Using IHC and/or ISH, GFP-positive signals were most frequently observed at the injection site in multiple cell types as well as in presumptive leukocytes in the draining and inguinal lymph nodes and spleen, with rare observations in the liver.

The biodistribution of BNT162b2 mRNA and its translation to spike protein were evaluated in BALB/cJrj mice. The highest ratios of BNT162b2 mRNA containing cells were in the injected muscle, liver, and spleen at 24 HPD. The lymph nodes also contained mRNA (<1%). Spike protein was detected in the injected muscle and lymph nodes but not in the spleen and liver tissue.

Finally, the metabolism of ALC-0315 (aminolipid) and ALC-0159 (PEG-lipid) was evaluated in vitro using blood, liver microsomes, S9 fractions, and hepatocytes from mice, rats, monkeys, and humans. The in vivo metabolism was examined in rat plasma, urine, feces, and liver samples collected during the PK study. In vitro and in vivo studies indicated ALC-0315 and ALC-0159 are metabolized slowly by hydrolytic metabolism of the ester and amide functionalities, respectively, across the species evaluated (in vitro and in vivo for ALC-0315 and in vitro only for ALC-0159).

### 2.6.4.2. Methods of Analysis

No methods of analysis have been validated to support GLP TK studies of components of BNT162b2; however, a qualified LC/MS method was developed to support quantitation of the two novel LNP excipients for the non-GLP IV PK study in rats (PF-07302048\_06Jul20\_072424).

### 2.6.4.3. Absorption

An intravenous rat PK study was performed using LNPs containing surrogate luciferase RNA, with the identical lipid composition as BNT162b2, to explore the disposition of ALC-0159 and ALC-0315 (Table 2.6.4-1, Study PF-07302048\_06Jul20\_072424; Tabulated Summary 2.6.5.3). The distribution of the LNP from the blood to the liver was rapid and essentially complete by 24 h, with <1% of the maximum observed plasma concentrations remaining (Figure 2.6.4-1). The liver appears to be the major site of drug uptake from the blood.

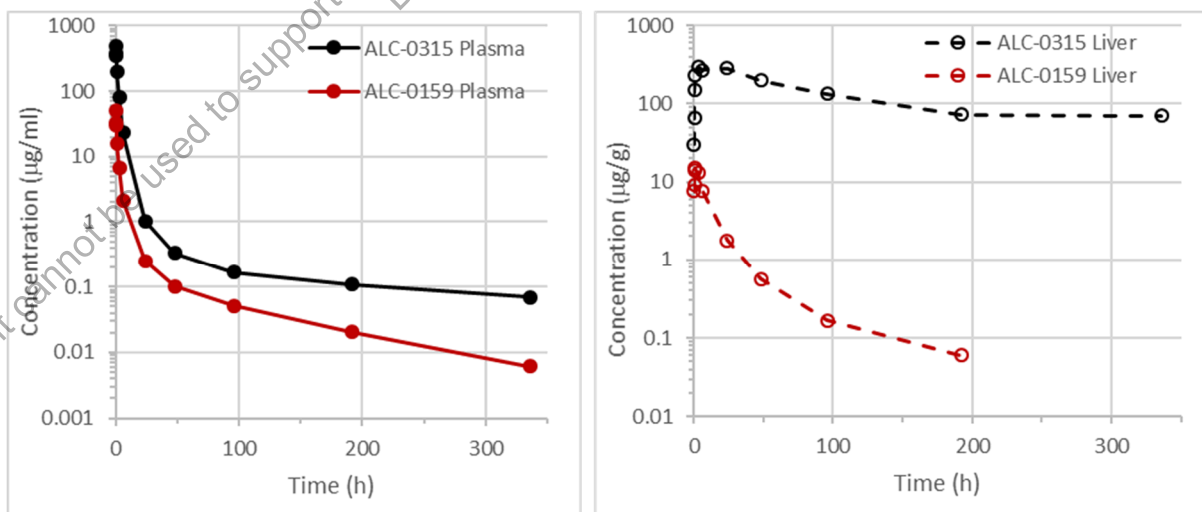
**Table 2.6.4-1. PK of ALC-0315 and ALC-0159 in Wistar Han Rats After IV Administration of LNPs Containing Surrogate Luciferase RNA at 1 mg/kg**

Analyte	Dose of Analyte (mg/kg)	Gender / N	t <sub>1/2</sub> (h)	AUC <sub>inf</sub> (µg•h/mL)	AUC <sub>last</sub> (µg•h/mL)	Estimated fraction of dose distributed to liver (%) <sup>a</sup>
ALC-0315	15.3	Male/3 <sup>b</sup>	139	1030	1020	60
ALC-0159	1.96	Male/3 <sup>b</sup>	72.7	99.2	98.6	20

a. Calculated as highest mean amount in the liver (µg)/total mean dose (µg) of ALC-0315 or ALC-0159.

b. 3 animals per timepoint; non-serial sampling.

**Figure 2.6.4-1. Plasma and Liver Concentrations of ALC-0315 and ALC-0159 in Wistar Han Rats After IV Administration of LNPs Containing Surrogate Luciferase RNA at 1 mg/kg**

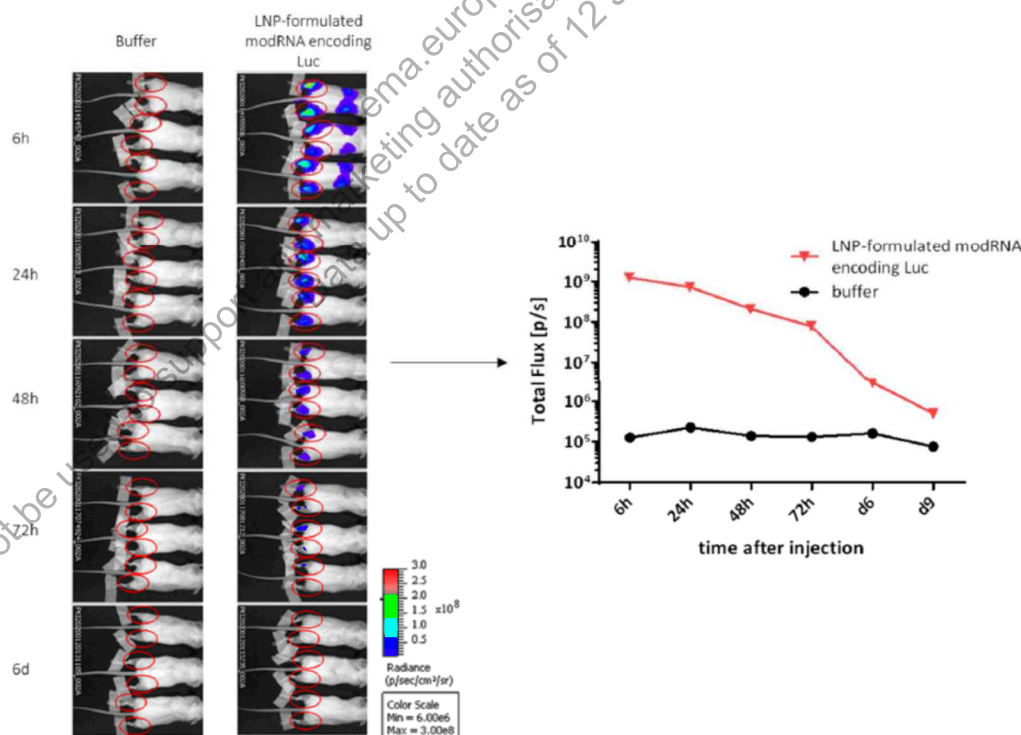


Pharmacokinetic studies have not been conducted with BNT162b2 and are generally not considered necessary to support the development and licensure of vaccine products for infectious diseases (WHO, 2005; WHO, 2014).

#### 2.6.4.4. Distribution

In an in vivo study in BALB/c mice (Study R-20-0072; Tabulated Summary 2.6.5.5A), the biodistribution of BNT162b2 was assessed using luciferase as a surrogate marker protein. RNA encoding luciferase was formulated like BNT162b2, with the identical lipid composition, and mice received IM injections of 1 µg each in the right and left hind leg (for a total of 2 µg) of LNP formulated- modRNA encoding luciferase. Luciferase protein expression was detected at different timepoints, by measuring the in vivo bioluminescence (Figure 2.6.4-2) after injection of luciferin substrate, at the site of injection and to a lesser extent in the liver. Distribution to the liver is likely mediated by LNPs entering the blood stream. The repeat-dose toxicity studies in rats showed no evidence of liver injury (Section 2.6.6.3). The luciferase expression at the injection site, the tissue with the highest bioluminescence, dropped to background levels after 9 days. As detailed in Section 2.6.4.3, following systemic (IV) administration the liver appears to be the major organ into which the LNPs distribute, this is consistent with the observations made following IM administration.

**Figure 2.6.4-2. Bioluminescence Emission in BALB/c Mice after IM Injection of an LNP Formulation of modRNA Encoding Luciferase**



These qualitative data are supported by a biodistribution study (Study 185350; Tabulated Summary 2.6.5.5B) carried out with LNPs with a comparable lipid composition as BNT162b2 but with a luciferase mRNA and a [<sup>3</sup>H]-CHE lipid radiolabel. Following IM administration to male and female Wistar Han rats at a dose of 50 µg (1.29 mg total lipid),

the greatest mean concentration was found remaining in the injection site at each time point in both sexes. Outside the injection site, the highest levels of radioactivity were observed in plasma at 1-4 HPD. Over 48 hours, the radiolabel distributed mainly to the liver, adrenal glands, spleen and ovaries, with maximum concentrations observed at 8-48 HPD. Total recovery of radioactivity (% of injected dose) outside the injection site was greatest in the liver (up to 18%) and was much less in the spleen ( $\leq 1.0\%$ ), adrenal glands ( $\leq 0.11\%$ ) and ovaries ( $\leq 0.095\%$ ). The mean concentrations and tissue distribution pattern were broadly similar between sexes.

An in vivo study evaluated the biodistribution of LNP-formulated modRNA encoding luciferase, using the same modRNA-LNP platform as the COVID-19 vaccine, in BALB/c mice (Study [R-23-0355](#); [Tabulated Summary 2.6.5.5C](#)). Following IM administration of 0.2  $\mu\text{g}$  or 1.0  $\mu\text{g}$  modRNA-LNP, animals were evaluated by in vivo BLI and tissues were evaluated for luciferase expression. Total luciferase expression in all organs of animals that received 1.0  $\mu\text{g}$  modRNA-LNP showed statistically significant higher luciferase expression 24 HPD compared with Day 6.

The injection site (muscle) and the closest draining lymph node (popliteal) were the main sites of luciferase expression for both modRNA-LNP dose levels, while additional draining lymph nodes on the right side of the body (where the injection was given), liver, and spleen all showed extremely low expression. At both dose levels, mRNA was distributed to the same main target organs, but the higher dose led to an increase in luciferase expression in lymph node tissue, suggesting potential influence of the modRNA dose on lymphatic drainage. BLI analysis also showed luciferase expression decreasing from Day 1 to Day 6 with the signal being detected mainly at the injection site.

To better understand the cellular distribution and protein expression of the modRNA-LNP platform of BNT162b2 in select tissues, a time course study was conducted in CD-1 male mice following IM injection of 1  $\mu\text{g}$  each in the right and left quadricep muscle (for a total of 2  $\mu\text{g}$ ) of GFP modRNA-LNP (Study [22GR161](#); [Tabulated Summary 2.6.5.16](#)). IHC identified cells that had taken up the modRNA-LNP and translated the mRNA to GFP, while ISH localized GFP mRNA in cells that had internalized the GFP modRNA-LNP.

GFP detected in the serum peaked at 6 HPD and gradually declined through 168 HPD. Using IHC (for protein) and ISH (for RNA) methods, GFP RNA and protein distribution was similar to that observed in the other biodistribution studies and was most frequent at the injection site, in the draining and inguinal lymph nodes, and spleen, with rare observations in the liver. GFP-positive signals were consistently detected in multiple cell types at the injection site: adipocytes, endothelium and perivascular connective tissue from thin-walled vessels (presumptive venules, capillaries, lymphatics), dermal fibroblasts, muscle connective tissues (epimysium, perimysium, and endomysium), rare myocytes, and mononuclear cells, as well as presumptive leukocytes in lymph nodes and spleen, and hepatocytes (for RNA only at 6 HPD). In muscle compartments in the injection site, GFP-positive signals were generally greatest at 6 and 24 HPD except in myocytes where the highest incidence occurred at 168 HPD. GFP-positive staining was not observed in the heart by either method.

IHC (for protein) and ISH (for RNA) staining generally overlapped; although, in spleen and liver, GFP-positive staining was only detectable by ISH and in inguinal lymph nodes, ISH labeling was present in multiple animals across time points but IHC labeling was only observed in 2 animals. Electron microscopy detected structures consistent with LNPs in spleen samples at 24 and 72 HPD, but not at 6 HPD; structures were not detected in the draining lymph nodes or injection site muscle samples.

Additionally, the biodistribution of BNT162b2 mRNA and its translation to spike protein in BALB/cJrj mice were evaluated (Study [R-23-0475](#); [Tabulated Summary 2.6.5.5D](#)). Following IM administration of 1 µg BNT162b2 in the right hind muscle, organs were collected 24 HPD for analysis. The highest ratios of BNT162b2 mRNA containing cells were in the injected muscle (2.1% to 15.9%), liver (3% to 8%), and spleen (1.4% to 3.8%) at 24 HPD. The mRNA was also present (<1%) in inguinal, popliteal, and axillary lymph nodes. Tissues from heart and lung showed ratios of BNT162b2 mRNA containing cells comparable to the saline control. For the brain, no conclusion could be drawn due to an unspecific binding of the probe used for BNT162b2 mRNA detection.

IHC-based analysis revealed the presence of spike protein in the injected muscle (with mean ratios of positive cells from 11% to 16%), and popliteal and inguinal lymph nodes (with mean ratios of positive areas from 0.3% to 1.7% and 0 to 1.6%, respectively) of all BNT162b2-injected mice. In one of the three mice, the axillary lymph node was also positive for spike protein expression with a mean positive area of 4%. There was no definitive evidence of spike expression in the brain tissue, spleen, liver, lung, and heart.

BNT162b2 mRNA was not translated into the spike protein in all cell types to which it was distributed. Translation appears to happen in several cell types in the muscle. In the lymph nodes, most of the cells expressing spike protein appeared to be macrophages. In contrast, cells located in the germinal centers, which were also positive for BNT162b2 mRNA, did not express spike protein. In the spleen, vaccine mRNA was restricted to the white pulp areas, which were strictly negative for spike protein. Finally, in the liver tissue, BNT162b2 mRNA appeared homogeneously distributed with no detectable translation into spike protein.

The biodistribution of the expression of the antigen encoded by the RNA component of BNT162b2 is expected to be dependent on the LNP distribution. Therefore, results of these biodistribution studies should be representative for BNT162b2, as the LNP-formulated luciferase-encoding modRNA had the same lipid composition.

#### **2.6.4.5. Metabolism**

Metabolism studies were conducted to evaluate ALC-0315 (aminolipid) and ALC-0159 (PEG-lipid). These novel lipids were evaluated for in vitro metabolic stability in CD-1/ICR mouse, Wistar Han and/or Sprague Dawley rat, cynomolgus monkey, and human liver microsomes, S9 fractions, and hepatocytes. ALC-0315 and ALC-0159 were stable (>82% remaining) over 120 min in liver microsomes and S9 fractions and over 240 min in hepatocytes in all species and test systems (Studies [01049-20008](#), [01049-20009](#), [01049-20010](#), [01049-20020](#), [01049-20021](#), and [01049-20022](#); [Tabulated Summaries 2.6.5.10A](#) and [2.6.5.10B](#)).



The metabolism of ALC-0315 and ALC-0159 was further evaluated (Study PF-07302048\_05Aug20\_043725; Tabulated Summaries 2.6.5.9, 2.6.5.10C, and 2.6.5.10D) in vitro using blood, liver S9 fractions, and hepatocytes from CD-1 mice, Wistar Han rats, cynomolgus monkeys, and humans and in vivo using the rat plasma, urine, feces, and liver from the PK study (Section 2.6.4.3). This study determined ALC-0315 and ALC-0159 are metabolized slowly and undergo hydrolytic metabolism of the ester and amide functionalities, respectively. This hydrolytic metabolism was observed across the species evaluated both in vitro and in vivo for ALC-0315 and in vitro only for ALC-0159 with no metabolites observed in vivo for ALC-0159, as shown in Figure 2.6.4-3 and Figure 2.6.4-4.

**Figure 2.6.4-3. Proposed Biotransformation Pathway of ALC-0315 in Various Species**

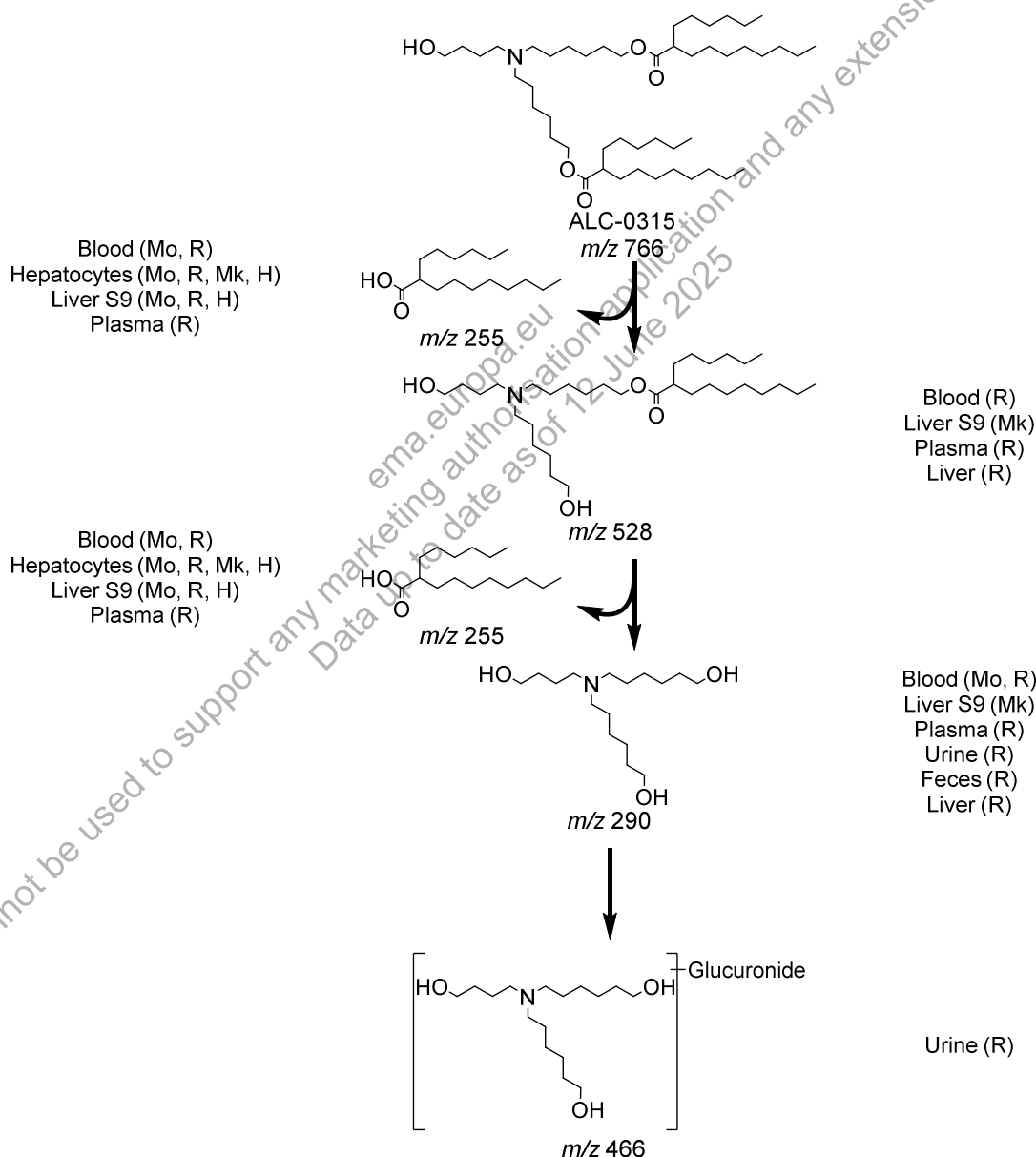
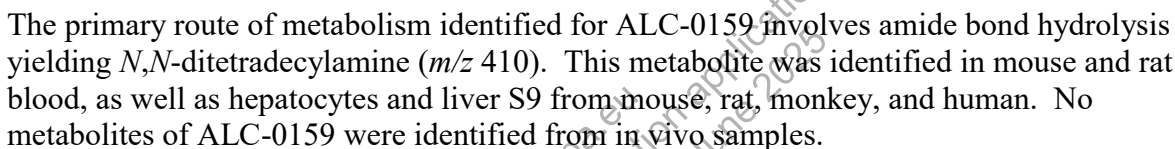


**Figure 2.6.4-4. Proposed Biotransformation Pathway of ALC-0159 in Various Species**



The other two lipids in the LNP are naturally occurring (cholesterol and DSPC) and will be metabolized and excreted like other endogenous lipids. As the protein encoded by the mRNA in BNT162b2 is expected to be proteolytically degraded and RNA is degraded by cellular RNases and subjected to nucleic acid metabolism, no RNA or protein metabolism or excretion studies will be conducted.

In the rat PK study (Section 2.6.4.3), there was no detectable excretion ALC-0315 and ALC-0159 in urine after IV administration of LNPs containing surrogate luciferase RNA at 1 mg/kg. The percent excreted unchanged in feces was ~1% for ALC-0315 and ~50% for ALC-0159. Metabolites of ALC-0315 were detected in the urine of rats (Figure 2.6.4-3). No excretion studies have been conducted with BNT162b2 for the reasons described in Section 2.6.4.5.

No PK drug interaction studies have been conducted with BNT162b2.

In the rat PK study, concentrations of ALC-0159 dropped approximately 8000- and >250-fold in plasma and liver, respectively, during this 2-week study. For ALC-0315, the elimination of the molecule from plasma and liver was slower, but concentrations fell approximately 7000- and 4-fold in two weeks for plasma and liver, respectively. Overall, the

apparent terminal  $t_{1/2}$  in plasma and liver were similar in both tissues and were 2-3 and 6-8 days for ALC-0159 and ALC-0315, respectively. The apparent terminal  $t_{1/2}$  in plasma likely represents the re-distribution of the respective lipids from the tissues into which they have distributed as the LNP back to plasma where they are eliminated.

Overall, it appears that 50% of ALC-0159 was eliminated unchanged in feces. Metabolism played a role in the elimination of ALC-0315, as little to no unchanged material was detected in either urine or feces. Investigations of urine, feces and plasma from the rat PK study identified a series of ester cleavage products of ALC-0315; this likely represents the primary clearance mechanism acting on this molecule, although no quantitative data is available to confirm this hypothesis. In vitro, ALC-0159 was metabolized slowly by hydrolytic metabolism of the amide functionality.

Biodistribution of the modRNA-LNP platform was initially assessed using luciferase or GFP expression as surrogate reporters formulated like the COVID-19 vaccine, with the identical lipid composition, or using a radiolabeled LNP-mRNA formulation. After IM injection of the modRNA-LNPs in mice, luciferase or GFP protein expression was mainly demonstrated at the site of injection and the draining lymph nodes. Biodistribution of the LNP was evaluated following IM administration of an LNP-mRNA formulation containing a radiolabeled lipid to rats. The percent of dose was also greatest at the injection site with total recovery of radioactivity next greatest in the liver and much lower in the spleen, adrenal glands, and ovaries.

The biodistribution of the vaccine was expected to be dependent on the LNP distribution, with the results representative for the vaccine RNA platform. This was confirmed by an additional biodistribution study administering BNT162b2 to mice. The highest ratios of BNT162b2 mRNA containing cells were in the injected muscle, liver, and spleen at 24 HPD with the lymph nodes also containing mRNA. Spike protein was detected in the injected muscle and lymph nodes and not observed in spleen and liver tissue.

#### 2.6.4.9. References

1. [World Health Organization. Annex 1. Guidelines on the nonclinical evaluation of vaccines. In: WHO Technical Report Series No. 927, Geneva, Switzerland. World Health Organization; 2005:31-63.](#)
2. [World Health Organization. Annex 2. Guidelines on the nonclinical evaluation of vaccine adjuvants and adjuvanted vaccines. In: WHO Technical Report Series No. 987, Geneva, Switzerland. World Health Organization 2014:59-100.](#)